

RESEARCH ARTICLE

10.1002/2015JC010972

Pairwise surface drifter separation in the western Pacific sector of the Southern Ocean

Erik van Sebille^{1,2,3}, Stephanie Waterman^{1,2,4}, Alice Barthel^{1,2}, Rick Lumpkin⁵, Shane R. Keating^{2,6}, Chris Fogwill¹, and Chris Turney¹

Key Points:

- Surface drifters are deployed in pairs south of New Zealand
- Dispersion between pairs is used to study mixing in the Southern Ocean
- Dispersion characteristics have generally lower magnitude than in North Atlantic

Supporting Information:

- Supporting Information S1
- Movie S1

Correspondence to:

E. van Sebille,
E.van-Sebille@imperial.ac.uk

Citation:

van Sebille, E., S. Waterman, A. Barthel, R. Lumpkin, S. R. Keating, C. Fogwill, and C. Turney (2015), Pairwise surface drifter separation in the western Pacific sector of the Southern Ocean, *J. Geophys. Res. Oceans*, 120, 6769–6781, doi:10.1002/2015JC010972.

Received 12 MAY 2015

Accepted 28 SEP 2015

Accepted article online 1 OCT 2015

Published online 17 OCT 2015

¹School of Biological, Earth and Environmental Sciences, University of New South Wales, Sydney, New South Wales, Australia, ²ARC Centre of Excellence for Climate System Science, Climate Change Research Centre, University of New South Wales, Sydney, New South Wales, Australia, ³Grantham Institute and Department of Physics, Imperial College London, London, UK, ⁴Department of Earth, Ocean and Atmospheric Sciences, University of British Columbia, Vancouver, British Columbia, Canada, ⁵NOAA/Atlantic Oceanographic and Meteorological Laboratory, Miami, Florida, USA, ⁶School of Mathematics and Statistics, University of New South Wales, Sydney, New South Wales, Australia

Abstract The Southern Ocean plays a critical role in global climate, yet the mixing properties of the circulation in this part of the ocean remain poorly understood. Here dispersion in the vicinity of the Southern Antarctic Circumpolar Current Front, one of the branches of the Antarctic Circumpolar Current, is studied using 10 pairs of surface drifters deployed systematically across the frontal jet and its flanks. Drifter pairs were deployed with an initial separation of 13 m and report their position every hour. The separation of the pairs over 7 months, in terms of their Finite-Scale Lyapunov Exponents (FSLE), dispersion, and diffusivity, is characterized and related to expected behavior from Quasi-Geostrophic (QG) and Surface Quasi-Geostrophic (SQG) theories. The FSLE analysis reveals two submesoscale regimes, with SQG-like behavior at scales below 3.2 km and mixed QG/SQG behavior at scales between 3.2 and 73 km. The dispersion analysis, however, suggests QG-like behavior for the smallest scales. Both dispersion and diffusivity appear isotropic for scales up to 500 km. Finally, there is no clear indication of a cross-jet variation of drifter dispersion.

1. Introduction

The ocean is full of eddies with many different scales [e.g., *Chelton et al.*, 2007]. These eddies impact the circulation and thereby the transport of heat, nutrients, and other so-called tracers of the circulation [Early et al., 2011]. They also play an important role in the material transport of particles such as planktonic organisms [Hellweger et al., 2014] and marine litter [van Sebille et al., 2012]. An improved understanding of how the eddying ocean mixes both particles and tracers can help quantify the impact of eddies on climate and ecosystems.

At the surface, drifting buoys can be used to study the dispersion of particles in a flow. For example, the separation of a pair (or triplet) of drifting buoys over time can be used to infer relative dispersion [e.g., *LaCasce*, 2008], which is a measure of the time rate of spread of a cloud of particles around its center of mass. Such an approach has been utilized to characterize the mixing of oceanic flows before, for instance, in the North Pacific [Kirwan et al., 1978; Davis, 1985], the North Atlantic [Ollitrault et al., 2005; Lumpkin and Elipot, 2010], the South Atlantic [Berti et al., 2011], the Nordic Seas [Koszalka et al., 2009], the Gulf of Mexico [Ohlmann and Niiler, 2001; LaCasce and Ohlmann, 2003; Poje et al., 2014], and the Mediterranean Sea [Lacorata et al., 2001; Haza et al., 2010; Schroeder et al., 2011, 2012]. These particle pair calculations are distinct from single-particle dispersion calculations [e.g., *Zhubas*, 2004], in that they indicate the relative stirring driven by the flow upon release of the pair, rather than the absolute dispersion from an arbitrary starting point. As such, these pair calculations reveal information about the stirring influence as a function of the scale of motion present in the flow (cf. *LaCasce* [2008] and section 2.2 below).

Dispersion in the Southern Ocean has received considerably less attention than in other parts of the world ocean [Trani et al., 2014]. Although single-particle dispersion studies have been undertaken in the region [Sallée et al., 2008], no experiment using paired drifters has been reported. Yet the Southern Ocean has very unique dynamics relative to that of the other basins, including elevated levels of eddy energy generally thought to enhance the rate of eddy mixing [e.g., *Stammer*, 1998], as well as strong zonal mean flows which

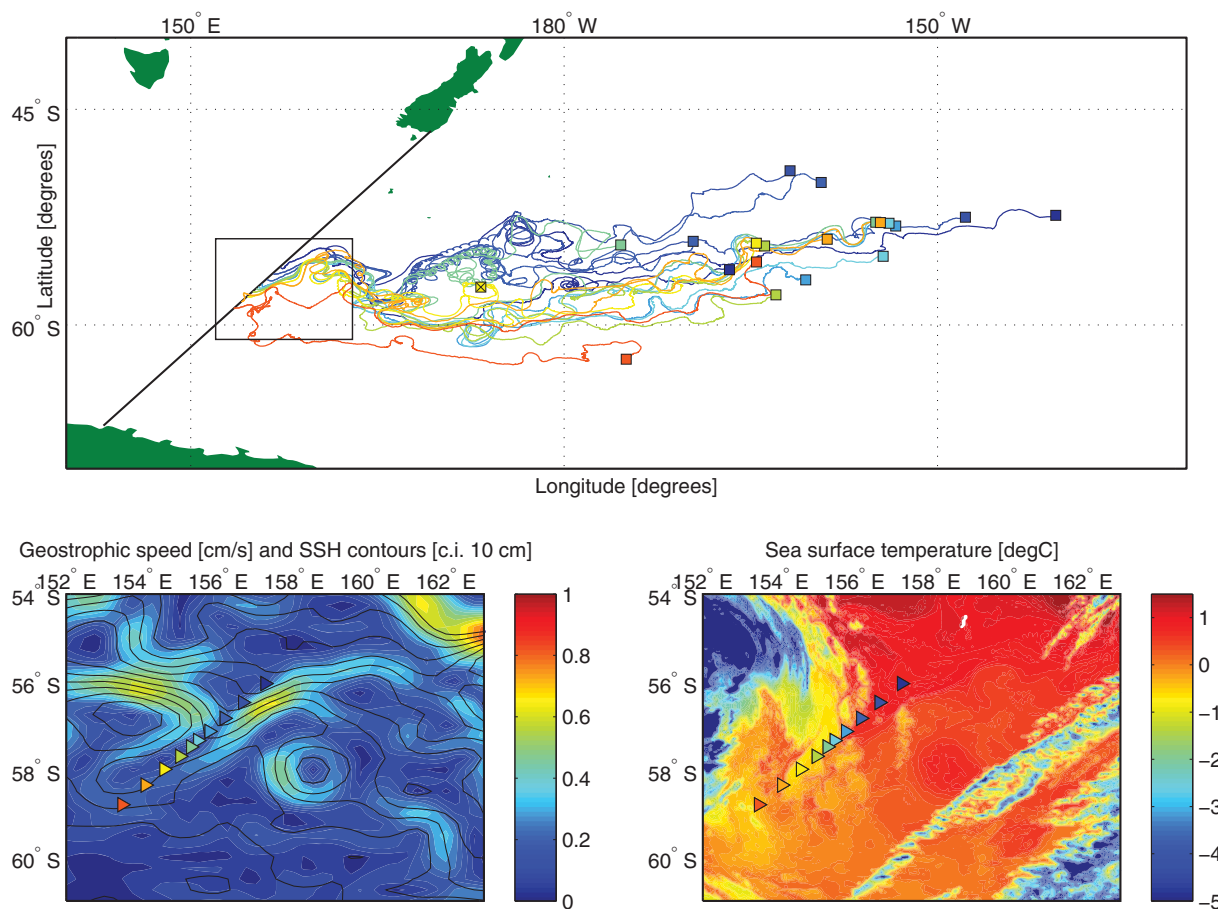


Figure 1. (a) Trajectories of the 20 drifters released during the 2013–2014 AAE expedition. Drifters were released along the black cruise track between New Zealand and Antarctica on 11 and 12 December 2013 and their trajectories until 31 July 2014 are shown here. Squares depict last locations, and the drifter with a cross on its endpoint is the only one that stopped reporting prematurely (on 27 April 2014). Drifters are color coded by release latitude, with the two drifters in a pair in the same color. (b) Altimetry data in a zoom of the release area (black box on Figure 1a), with triangles showing the release locations of the drifter pairs, lines the sea surface height contours on 11 December 2013, and the coloring the associated geostrophic speed. (c) Same as Figure 1b, but for sea surface temperature data from MODIS Aqua. The data shown are an 8 day binned average starting on 11 December 2013.

may act to suppress the eddy mixing rate [Ferrari and Nikurashin, 2010; Naveira Garabato *et al.*, 2011; Klocker and Abernathy, 2014], and a much smaller Rossby scale of deformation L_d [Chelton *et al.*, 1998]. Given that the Southern Ocean plays a key role in global climate and ocean circulation [Rintoul and Naveira Garabato, 2013], a better understanding of dispersion and mixing in this part of the world ocean is critical [Mazloff *et al.*, 2010].

During the 2013–2014 Australasian Antarctic Expedition (AAE) en route between New Zealand and Commonwealth Bay, we deployed 10 pairs of surface drifters (Figure 1) with the goal of characterizing dispersion and eddy diffusivity across an Antarctic Circumpolar Current (ACC) front. We targeted the deployment of the 10 pairs to span the Southern Antarctic Circumpolar Current Front (SACCF) and its flanks, a circulation feature associated with strong flows and an energetic eddy field, and believed to be associated with locally elevated surface mixing [Sallée *et al.*, 2011]. Here we use the data obtained from the trajectories of the surface drifters over a 7 month period to study pairwise dispersion in this highly dynamic, influential, and relatively understudied part of the global ocean.

2. Data and Theory

2.1. Drifter Data

The main data set used in this study is the trajectories of 10 pairs of GPS/Iridium surface drifter buoys deployed during the AAE in collaboration with NOAA [Ollitrault *et al.*, 2005; Lumpkin and Pazos, 2007;

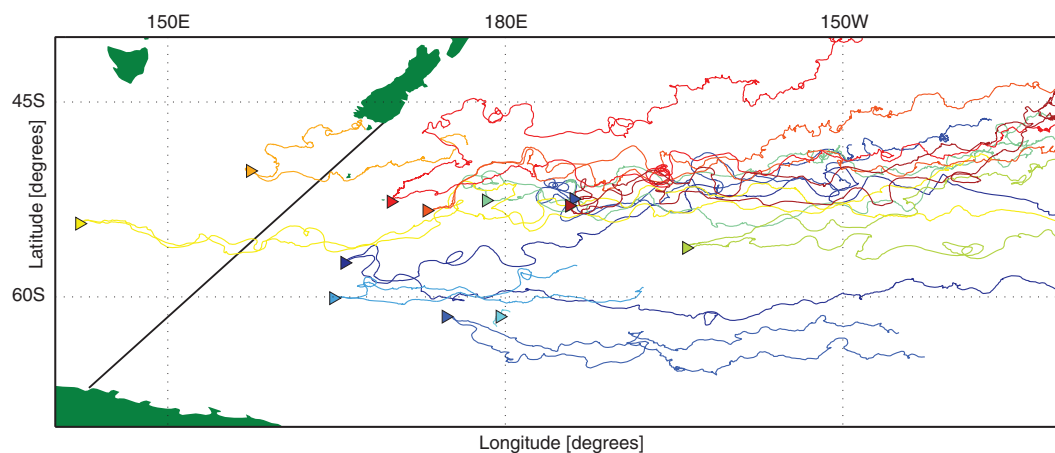


Figure 2. Trajectories of the 36 drifters that form the set of chance pairs, which augment our analysis of the set of drifters deployed during the 2013–2014 AAE. To be included, we required the chance pairs to get within 10 km of each other in the area (140°E – 160°W , 60°S – 45°S). Triangles are the start locations of the chance pairs, and the dashed line is the cruise track along which the AAE drifters were deployed.

Lumpkin and Elipot, 2010]. The drifters are drogued at 15 m depth using a sea anchor that deploys within minutes after the drifters are released. Within each pair, the two drifters were deployed at the same time from either side of the stern of the ship (13 m apart) while the ship was steaming ahead at approximately 10 knots (18.5 km/h). The analysis here focuses upon the first 7 months of the drifters' separation, which covers separation distances from scales of order 100 m to scales of order 1000 km. As such, the drifters sampled the flow field on scales much larger than the largest rings and meanders.

The drifter pairs were deployed on a straight line along the cruise track between approximately (56.0°S , 157.2°E) and (58.8°S , 153.5°E) (Figure 1) over a 25 h period starting on 11 December 2013. Our deployment strategy was to use near-real-time altimetry data to continuously track the location of the SACCF front so that half of the drifters (five pairs) could be deployed to the north of the SACCF and half to the south. However, postdeployment analysis of satellite altimetry (processed by AVISO) and 8 day average sea-surface temperature data (from MODIS Aqua) revealed that the SACCF developed a large meander at the time of deployment, so that pairs 1 and 2 were deployed just north of the frontal core, pairs 3 and 4 were deployed inside it, and pairs 5–10 were deployed south of the core (Figures 1b and 1c).

The drifters have since reported back their location via Iridium satellites, which have been processed into hourly locations at the NOAA AOML GDP Drifter Data Assembly Center (<http://www.aoml.noaa.gov/phod/dac/dacdata.php>). One drifter (part of pair 8) stopped reporting its position on 27 April 2014, but all other drifters were still operational by 31 July 2014, providing 230 days of drifter data for 19 out of the 20 drifters, and 137 days of data for drifter pair 8.

After deployment, all 20 drifters moved eastward along the SACCF (Figure 1a and movie in supporting information). In the 7 months after deployment, they spread out over a region spanning approximately 30° in longitude and 15° in latitude, and achieved a maximum separation of almost 1400 km. The trajectories show indications of inertial motions, as well as signatures associated with the capture of drifters in meso-scale eddies, particularly around 170°E (Figure 1).

In addition to the 10 dedicated pairs, we also consider the separation of chance drifter pairs, defined as pairs of surface drifters similar to the ones deployed in the AAE that happened to come close to each other in the region of interest in the historical data set of drifters deployed since the 1980s. One of the advantages of incorporating chance pairs is that they are an independent data set that can test the extent to which the statistics from the AAE drifters are stationary and representative of those derived over a larger temporal and spatial window. We define chance pairs in this study as any pair of drifters that came within 10 km of each other within a 6 h window in the region (140°E – 160°W , 65°S – 50°S). This definition yielded 12 chance pairs in the historical data set, whose trajectories forward in time from the moment they reach their minimum separation are shown in Figure 2. The fact that only 12 pairs of drifters have ever come within 10 km of each other in this vast area of ocean highlights the utility of dedicated pair deployments.

2.2. Quantifying Mixing

2.2.1. Pair Dispersion

Single-particle dispersion theory [Taylor, 1921] is traditionally used to analyze the displacement of a particle from a fixed position under the action of random turbulent motions. To investigate the spread of a cloud of particles about their center of mass by the flow, it is more appropriate to analyze dispersion among pairs of particles. This results in a relative diffusivity K that depends on the pair separation D , thus characterizing the mixing properties of the circulation as a function of the length scales present in the flow:

$$K(D) = \frac{1}{2} \frac{d}{dt} (D^2).$$

The relative diffusivity at each separation scale D will depend on the kinetic energy present in the flow at that scale. If the kinetic energy spectrum E is proportional to k^{-n} over some range of isotropic wavenumbers k , the scale dependence of the relative diffusivity undergoes a transition at $n = 3$ [Bennett, 1984]. For steep spectral slopes $n \geq 3$, the relative diffusivity K is proportional to D^2 , implying that pairwise dispersion D^2 increases exponentially with time t . This is the situation when a particle pair undergoes straining by a smooth velocity field [Batchelor, 1952] or when the pair separation is dominated by eddies much larger than the separation distance. In this case, the dynamics are said to be *nonlocal* in scale, meaning that the relative diffusivity at a given scale is controlled by stirring on a different scale.

By contrast, for shallow spectral slopes $n \leq 3$, the relative diffusivity can be shown to scale as $K \propto D^{(n+1)/2}$. In this case, the relative diffusivity for particle pairs separated by a distance D is controlled by stirring by eddies of the same scale; this is referred to as *local* dynamics. For the case of $n = 5/3$, which describes forced-dissipative 3-D turbulence, we expect D^2 to vary as t^3 , with diffusivity following Richardson's four-thirds power law, $K \propto D^{4/3}$ [Richardson, 1926].

The most widely studied model for mesoscale ocean dynamics is given by 2-D Quasi-Geostrophic (QG) turbulence theory [Pedlosky, 1987; Salmon, 1998; Vallis, 2006]. In QG dynamics, we expect three distinct scale-dependent dispersion regimes [LaCasce, 2008]. For pair separation D smaller than the Rossby deformation radius L_d , we expect the spectral slope n to equal 3. As such, we expect the pairwise dispersion D^2 to increase exponentially with time t . By contrast, for scales between L_d and the biggest eddies in the flow field, we expect the spectral slope n to be greater than or equal to $5/3$, and D^2 to vary as t^3 with diffusivity following Richardson's four-thirds law. Finally, for separations at scales larger than the largest eddies in the flow field, a purely diffusive random walk regime is expected with $D \propto t$. In this regime, K is expected to be constant and equal to twice the single-particle (absolute) diffusivity ($K = 2K_{obs}$). For drifter pairs released in a 2-D QG turbulent flow and whose separation is expected to evolve from a distance smaller than the Rossby deformation radius through L_d and finally to distances larger than the largest eddies in the flow field, we thus expect pairwise dispersion D^2 to first increase exponentially with time (the "exponential regime"), then to vary as t^3 (the "Richardson regime"), and finally to scale linearly with time (the "diffusive regime").

In the upper ocean, surface buoyancy dynamics can dominate the evolution of the flow [Lapeyre and Klein, 2006]. In this case, Surface Quasi-Geostrophic (SQG) theory may be a more appropriate description for the drifter pair behavior. SQG theory suggests that the kinetic energy spectral slope $n = 5/3$ for scales less than L_d [Held et al., 1995]. This would imply that Richardson's law is valid from the subdeformation scale to L_d , a range of scales where 2-D QG turbulence would predict exponential growth of dispersion with time. Two-dimensional QG and SQG dynamics can be present simultaneously, with a transition from $n = 3$ to $n = 5/3$ at some intermediate scale between the submesoscale and L_d [Tulloch and Smith, 2009]. It is unclear which theory can be consistently observed in surface drifter dispersion at small scales, as previous studies [Ollitrault et al., 2005; Koszalka et al., 2009; Lumpkin and Elipot, 2010; Poje et al., 2014] differ in their conclusions.

2.2.2. Finite-Scale Lyapunov Exponents

An alternative approach to characterizing the mixing properties of the flow from drifter pair separations is to calculate the Finite-Scale Lyapunov Exponents (FSLE), defined as the exponential growth rate of the drifter separation as a function of separation distance [e.g., LaCasce, 2008]. The FSLE λ associated with scale D is calculated from the shortest time $\tau(D)$ required for the pair separation to increase by a factor of $r > 1$ according to

$$\lambda(D) = \frac{\ln r}{\tau(D)}$$

Dispersion regimes can then be identified from the exponent α in the scaling of $\lambda \propto D^\alpha$: in the exponential regime, λ is constant so $\alpha = 0$; in the Richardson regime, $\alpha = -2/3$; and in the diffusive regime, $\alpha = -2$ [LaCasce, 2008].

As the FSLE method averages time at fixed distances rather than distances at fixed times (used in relative dispersion), it is a more appropriate metric to highlight mixing characteristics occurring at specific spatial scales. In addition, given that relative dispersion calculations tend to become less robust with increasing time due to a decreasing number of pairs being included in the calculation, due to drifters dying or losing their drogues. By contrast, FSLE calculations become increasingly robust with increasing separation distance as more pairs can be included in the calculation [Lumpkin and Elipot, 2010], and so it is an attractive complementary mixing metric to consider especially at long times. While it has recently been shown that drifter position errors can contaminate FSLE results on scales up to 60 times larger than those errors [Haza et al., 2014], this contamination is not expected to significantly affect our results, as the GPS positions of our drifters have errors of ~ 1 m.

In this particular data set, the FSLE analysis has an additional advantage of being insensitive to the inclusion/omission of one outlier pair, which is not the case for the dispersion versus time analysis (see section 3.2). As a consequence, in what follows, we present results from the FSLE analysis first. We will then use the characteristics of the different dispersion regimes identified from the FSLE analysis to interpret the more complicated regime transitions in the dispersion-versus-time analysis. It should be noted however that, although the FSLE results have the potential to offer useful guidance in identifying regimes in the dispersion characterization, it is not necessarily expected that the two analysis methods will identify consistent dynamic regimes in the flow. This is because the FSLE analysis separates the flow based on the spatial scales of motion, whereas the dispersion-versus-time analysis separates the flow based on time scales. As a consequence, the dispersion metric tends to mix different scales of motions at all times, whereas the scale-dependent FSLE isolates each scale of motion from the other scales. While the FSLE analysis has the advantages of being intrinsically defined as a function of length scale and less sensitive to the outlier pair, there is emerging evidence that inertial oscillations can potentially contaminate the FSLE results on very small scales (F. J. Beron-Vera and J. H. LaCasce 2015). As the debate on the merits and best usages of both metrics is still ongoing, here we consider both and highlight both the similarities and differences in their characterization of the mixing properties of the flow.

3. Results

3.1. Finite-Scale Lyapunov Exponent Analysis

Following Lumpkin and Elipot [2010], we compute the Finite-Scale Lyapunov Exponents (FSLEs, see also section 2.2) for the dedicated drifter pairs deployed during the AAE and average over all 10 pairs (Figure 3). As suggested by the sensitivity analysis proposed by Haza et al. [2008] and Lumpkin and Elipot [2010], we chose $r = 1.25$, a compromise between minimizing noise in the slope fits and maintaining resolution in the FSLE estimates as a function of scale. The analysis is in this case not very sensitive to this choice for r , as the slopes in the FSLE analysis are statistically indistinguishable for all values of $r < 1.50$ (Figure 4).

The FSLE analysis shows that the AAE drifter pairs exhibit several distinct scaling regimes $\lambda \propto D^\alpha$, depending on the drifter separation D (Figure 3). This is similar to the behavior of drifter pairs in other regions of the world ocean reported by, for example, LaCasce and Ohlmann [2003], Ollitrault et al. [2005], Koszalka et al. [2009], and Lumpkin and Elipot [2010]. However, the length scales of the various regime transitions, as well as the scaling exponents α for each of the regimes, vary considerably between all studies, and here too we find that the quantitative fits show some unique features relative to those reported in the past.

The FSLE results in this region (Figure 3) suggest at least two regime transitions over a range of separations spanning 0.1–1000 km. These are observed to occur at separation scales of approximately 1–5 and 50–100 km, respectively, with larger values of α (i.e., steeper slopes of $\log(\lambda)$ versus $\log(D)$ or equivalently slower rates of particle separation) characterizing the drifter behavior at the small and large scales relative to the middle separation scale. We quantify the transitions by assuming each of these three regimes are described

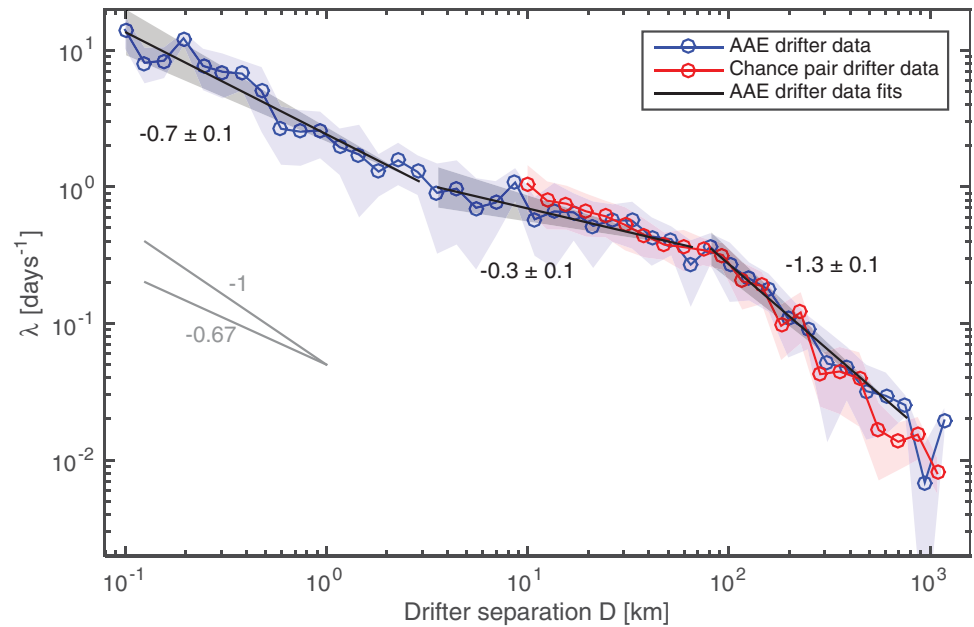


Figure 3. Finite-Scale Lyapunov Exponents for the 10 AAE drifter pairs. Blue circles are mean values as a function of drifter separation; the light blue envelope is the bootstrapped 95% confidence interval. The red lines, circles, and envelope are for the 12 chance pairs. Black lines are least squares power law fits for three regimes. Breakpoints between regimes were determined by minimizing the standard errors in the power law fits. The grey envelopes denote the 95% confidence intervals on the best fits, and the numbers give the slope parameters and their 95% confidence intervals. The two grey lines on the left are the slopes for ballistic ($\alpha = -1$) and Richardson ($\alpha = -2/3$) behavior.

by a constant value of α , and then select the length scales of regime transition so as to minimize the summed standard error in the estimation of the three slope values computed by a least squares fit. The results of these calculations give a dependence of λ on D of the form $\lambda \propto D^{-0.7 \pm 0.1}$ (i.e., $\alpha = -0.7$, with a 95% confidence interval on the least squares fit of the slope of 0.1) for separations less than 3.2 km, a dependence of λ on D of the form $\lambda \propto D^{-0.3 \pm 0.1}$ for intermediate separations in the range of 3.2–73 km \sim

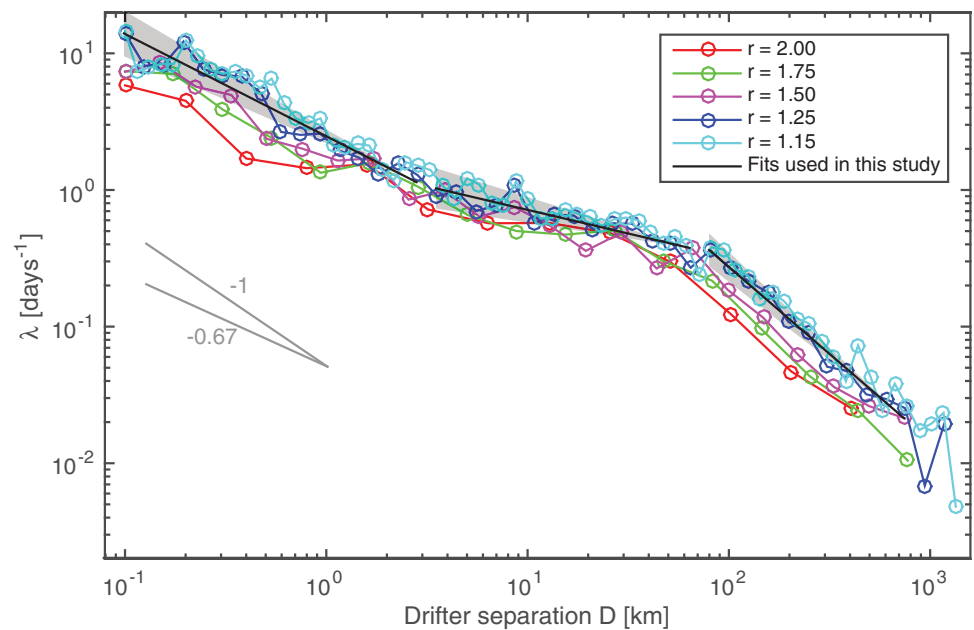


Figure 4. Analysis of the sensitivity of the results of the FSLE analysis to our choice of the parameter r . Following the method by Haza *et al.* [2008] and Lumpkin and Elipot [2010], the FSLE analysis is performed with different values of r . The smallest value where the slope does not change is then chosen; in this case as $r = 1.25$. The black lines with grey envelopes are the best fits of the $r = 1.25$ line from Figure 3.

$2 L_d$, and finally a dependence of λ on D of the form $\lambda \propto D^{-1.3 \pm 0.1}$ for large separations greater than 73 km $\sim 2 L_d$.

Comparing these results to theoretical expectations, we note first that for small separation scales, the observed behavior is consistent, within the 95% confidence interval, with Richardson regime behavior (characterized by $\alpha = -2/3$) as predicted by SQG theory. For intermediate scales (i.e., $3.2 \text{ km} < D < 73 \text{ km} \sim 2L_d$), however, the observed slope of $\alpha = -0.3 \pm 0.1$ is larger than the $\alpha = -2/3$ slope expected in a SQG regime, and smaller than the $\alpha = 0$ fit expected for exponential separation in a QG regime. The steepening of the λ versus D slope for larger ($D < 73 \text{ km} \sim 2 L_d$) scales is consistent with QG predictions, but we note that quantitatively the slope that we find ($\alpha = -1.3 \pm 0.1$) is significantly less steep than expected in the diffusive regime ($\alpha = -2$). This implies that we see significantly faster dispersion for these larger scales than predicted by QG theory.

Our results can be compared to previous observations of pairwise dispersion in other parts of the world ocean. We note first that the Richardson regime-like behavior we see at the smallest resolved scales agrees with the smallest-scale regime reported by *Schroeder et al.* [2012] in the northwestern Mediterranean and *Poje et al.* [2014] in the Gulf of Mexico. In the case of the former, however, this regime extends to scales up to 5 km (versus up to 3.2 km in the AAE data). We speculate that the smaller range of scales for which Richardson regime-like behavior applies in our study region may reflect the influence of a smaller deformation radius at these latitudes. Richardson regime behavior at small (subdeformation scale) scales, however, is not universal. *Lumpkin and Elipot* [2010], for example, found ballistic ($\alpha = -1.0$) behavior for dispersion in the North Atlantic, extending to separations up to 8 km, although it is worth noting that the drifters used in this study were not GPS tracked but rather tracked using the Argos location system, and as such had considerably larger spatial errors.

For scales between 3.2 and 73 km, approximately twice the Rossby radius of deformation, the slope of $\alpha = -0.3 \pm 0.1$ that characterizes the AAE data differs from the exponential regime behavior ($\alpha = 0$) typically found for the larger of the submesoscale ranges. For example, *Lacorata et al.* [2001] report the suggestion of exponential behavior for scales below 50 km in the Adriatic Sea; *Berti et al.* [2011] found scale-independent behavior in the southwestern Atlantic Ocean for scales between 500 and 8 km, and then again between 10 and 100 km with a step between these two regimes. It is unclear why the FSLE analysis in this AAE data set does not show an exponential regime.

Finally, the regime of drifter behavior seen here for the larger mesoscale range of scales ($\alpha = -1.3 \pm 0.1$) is typical: it has been observed by *Lumpkin and Elipot* [2010] and also confirmed in ocean models by *Poje et al.* [2010]. Here we note however that the transition to this regime of behavior occurs at a significantly smaller scale in our AAE data than in the North Atlantic data set analyzed by *Lumpkin and Elipot* [2010] (73 km compared to 240 km). The early onset of the $\alpha = -1.3$ regime in this part of the Southern Ocean does not seem to be an anomaly particular to the AAE drifter set but rather a general property of the flow in the region between 55°S and 65°S, as a similar result is seen in the analysis of the 12 chance pairs (red lines in Figure 3), whose behavior closely follow that of the AAE drifters and is always within the error bars of the AAE pair FSLE. The agreement suggests that our results derived from the AAE drifters on scales larger than 10 km are broadly representative of the southwest Pacific sector of the Southern Ocean, and that biases such as seasonal effects are limited. Again we speculate that the smaller scale for regime transition may reflect the influence of a smaller deformation radius at these latitudes.

3.2. Dispersion Analysis and the Effect of an Outlier Pair

An alternative characterization of the flow's mixing regimes can be derived from an analysis of the dispersion (the ensemble-averaged square of drifter separation, D^2) versus time, presented for the AAE drifter data in Figure 5. As noted in section 2, the characterization of dispersion reveals the existence of an anomalous outlier drifter pair that has a dispersion of 2 orders of magnitude higher than all other pairs for the first 10 days after release (dashed lines in Figure 5). The inclusion or omission of this pair impacts the mean pair dispersion evolution considerably in this period (dashed thick versus solid thick lines in Figure 5).

Given the resulting ambiguity in the interpretation of the dispersion results, we start by evaluating the applicability of the regime behaviors and transitions identified in the FSLE analysis to the dispersion versus

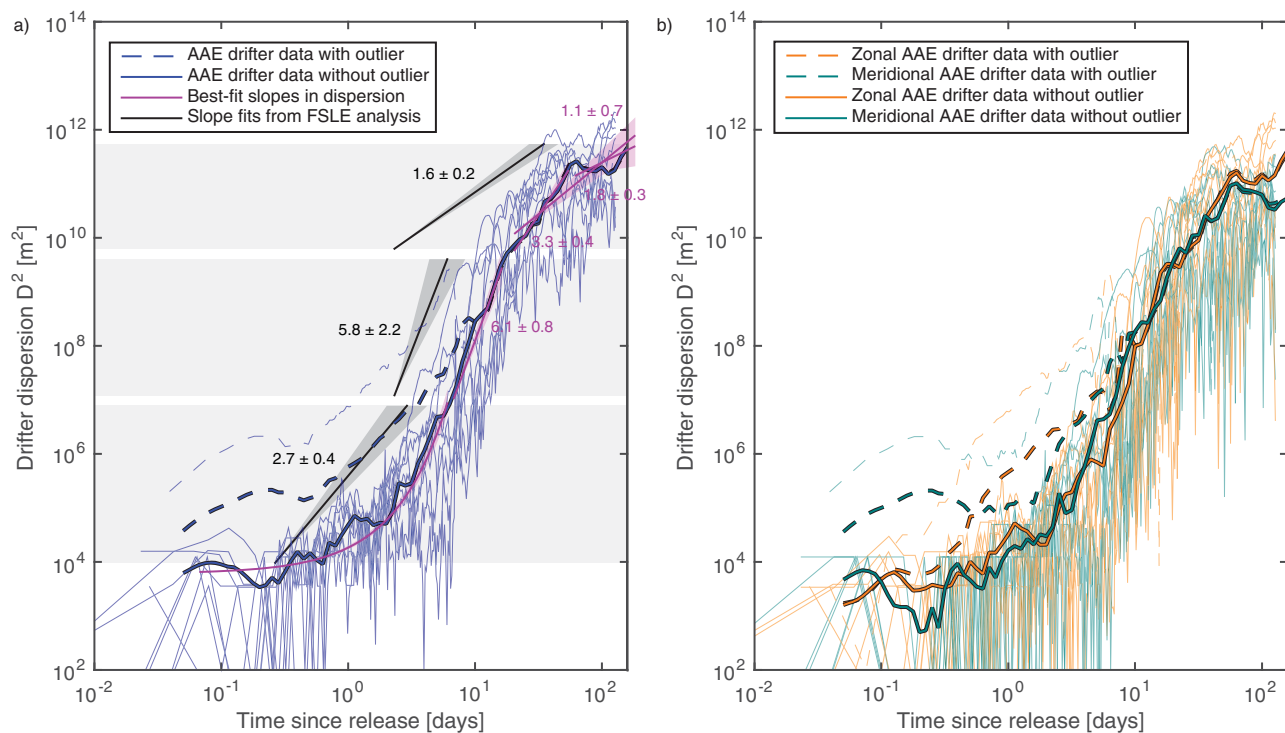


Figure 5. Dispersion versus time characteristics of the surface drifters on a log-log scale. (a) Total dispersion and (b) dispersion separated in zonal and meridional components. Each pair is represented by a thin line. The outlier pair that has much higher dispersion in the first 10 days is shown by the thin dashed line. In both plots, the mean of the 10 pairs is shown by the thick dashed lines, while the mean of the set excluding the outlier pair is shown by the thick solid lines. In Figure 5a, the best fit slopes to the solid thick lines are shown as purple lines. Light purple shading shows the 95% confidence intervals. The slope parameters for the power law slope fits are given. The dispersion-versus-time slopes implied from the FSLE analysis are shown as black lines with dark grey shading denoting their confidence intervals, and are offset to ease comparison. Light grey bands denote the dispersions equivalent to the separation ranges for each of the three regimes identified in the FSLE analysis (Figure 3).

time behavior. We note that if the FSLE follows $\lambda \propto D^\alpha$, then the dispersion follows $D^2 \propto t^{-2/\alpha}$ [LaCasce, 2008]. Thus, one can infer the rate of change of dispersion implied by the best fit exponents α of the FSLE analysis and compare it to the observed dispersion. This is done in Figure 5a where the dispersion slopes inferred from the FSLE analysis are shown in black for each of the three regimes identified (equivalent regime spans in time denoted by light grey areas).

We find that the FSLE versus dispersion analysis characterization of the drifters' separation is in agreement for some ranges of length and time scales but not for others. As noted earlier, these discrepancies are not unexpected given the different ways the two diagnostics average over space and time. Furthermore, we find that the correspondence between the two characterizations can be very sensitive to the inclusion/omission of the outlier pair.

For small separations/times, specifically separations between 100 m and 2.8 km corresponding to the first 3.5 days (with outlier pair) or 6.3 days (without outlier pair) of mean dispersion, the dispersion does not appear to follow a power law consistent with Richardson regime behavior identified via the FSLE analysis. Instead, dispersion appears to increase exponentially for these times. This is especially so for the case of the mean without the outlier pair (solid thick blue/black line in Figure 5a), which shows an exponential increase in dispersion for the first 5 days with a growth rate of $1.5 \pm 0.1 \text{ day}^{-1}$. Recalling that an exponential regime implies an $\alpha = 0$ fit in the FSLE analysis (Figure 3), the two mixing diagnostics clearly do not agree in this range of separations/times.

By contrast, we find good agreement between the two diagnostics for the larger of the two submesoscale regimes identified in the FSLE analysis, and applicable to separations ranging from 3.2 to 73 km and corresponding to times between 4.0 and 16 days (with outlier) or between 6.8 and 16 days (without outlier) after release. Specifically, the best fit dispersion power law in this range of times is statistically indistinguishable

from that expected from the FSLE analysis if the outlier is excluded. When the outlier pair is included in the analysis, the dispersion appears to evolve slightly slower than the FSLE analysis suggests.

Finally, in the mesoscale regime for separations greater than 73 km, the FSLE slope of $\alpha = -1.3 \pm 0.1$ again does not agree well with the dispersion analysis results. While the mean time rate of change of dispersion between 20 and 200 days is similar to that implied by the FSLE analysis, the dispersion behavior seems to identify an additional regime transition, after 65 days and at a scale of ~ 500 km. For shorter times, the dispersion slope is steeper (implying a flatter slope in the FSLE analysis), while after 65 days the rate of change of dispersion slows. It is worth noting that while this regime transition seen at 65 days also occurs in the zonal component of the dispersion, it is particularly evident in the meridional component (thick green/black line in Figure 5b). Before that time, the dispersion (especially when the outlier pair is removed) is fairly isotropic, with the mean zonal and meridional dispersion curves appearing similar. It seems therefore that large-scale anisotropy in this data set only emerges after 65 days.

Closer analysis of the outlier pair trajectories (Figure 6) shows that this pair's separation was almost an order of magnitude larger at the first location fix compared to that of all other pairs. This first location fix was almost an hour after the deployment, and the separation of the outlier pair at that time was 450 m. Such rapid initial separation, although not impossible, is quite extraordinary. In our hourly data set of 10 pairs from the AAE expedition, there were 1450 instances where the separation of a pair was less than 1 km, and out of these instances, there were only eight when the separation grew by more than 450 m in an hour, indicating that the chance of such a large rate of separation when the drifters are still so close is less than 1%. On the other hand, we have no apparent reason to discard this particular data point (for example, because something went wrong at the deployment such as nonsimultaneous deployment or observing that one of the drogues did not deploy quickly enough). As such it could well be that this outlier pair has sampled a strongly divergent flow. Unfortunately, the altimetry data do not have sufficiently high resolution to test this hypothesis.

3.3. Drifter Diffusivity Analysis

From the dispersion versus time behavior, we estimate the diffusivity (the rate of change of separation, $1/2 dD^2/dt$) as a function of separation D (Figure 7). Both the AAE drifter data and the chance pair data show a reasonably close fit with the theoretical Richardson $D^{4/3}$ power law, although the exponential fit seems to be larger (approximately 1.6) for $D < 20$ km. Further, both data sets appear to asymptote to a diffusivity magnitude (10^4 – 10^6 m²/s) in agreement with previous studies [e.g., Koszalka *et al.*, 2009; Poje *et al.*, 2014]. However, there is no obvious relationship with the three or four different regimes of behavior identified in the FSLE and dispersion analysis. Further, while the magnitude of the diffusivity is in good agreement with that found in the North Atlantic [Ollitrault *et al.*, 2005], here we find that the diffusivity continues to increase even beyond scales much larger than the largest eddy scale (order 100 km), where some theories predict random walk behavior and constant diffusivity with separation distance.

One hypothesis for why we do not observe a purely diffusive regime (with constant diffusivity) even at scales larger than the expected large eddy scale is the influence of the background flow, in particular, the shear within and between the different jets of the ACC. It has been shown that the strong anisotropy of the ACC causes material transport in this region, which is dominated by zonally elongated eddies and transient jets, which can have length scales much larger than $O(100)$ km [Kamenkovich *et al.*, 2015]. As such, it seems plausible that the relevant eddy scale for the onset of a diffusive regime in the zonal direction here is very large. However, separation of the diffusivity into its zonal and meridional components (Figure 7b) does not show any clear anisotropy in the AAE data set on any scale, and as such there is no indication that very large zonally elongated eddies are having a strong influence on the dispersion characteristics.

The analysis of diffusivity is also interesting because it shows no significant change in diffusivity on short length scales between the SACCF jet core and jet flanks, a conclusion that is reached from the observation that there is no apparent segregation of the drifter diffusivity as a function of release latitude (Figure 7). While this is expected for large separation distances, when the drifters cannot be expected to be in the same flow type, this is somewhat surprising for length scales smaller than 20 km. When diffusivity slopes for $D < 20$ km are fitted for each pair using the power law $dD_i/dt = a_i \left(\frac{D_i}{D_0}\right)^{1.6}$, where $D_0 = 13$ m is the initial separation, we find no significant relation between the fit parameter a and the release location or release

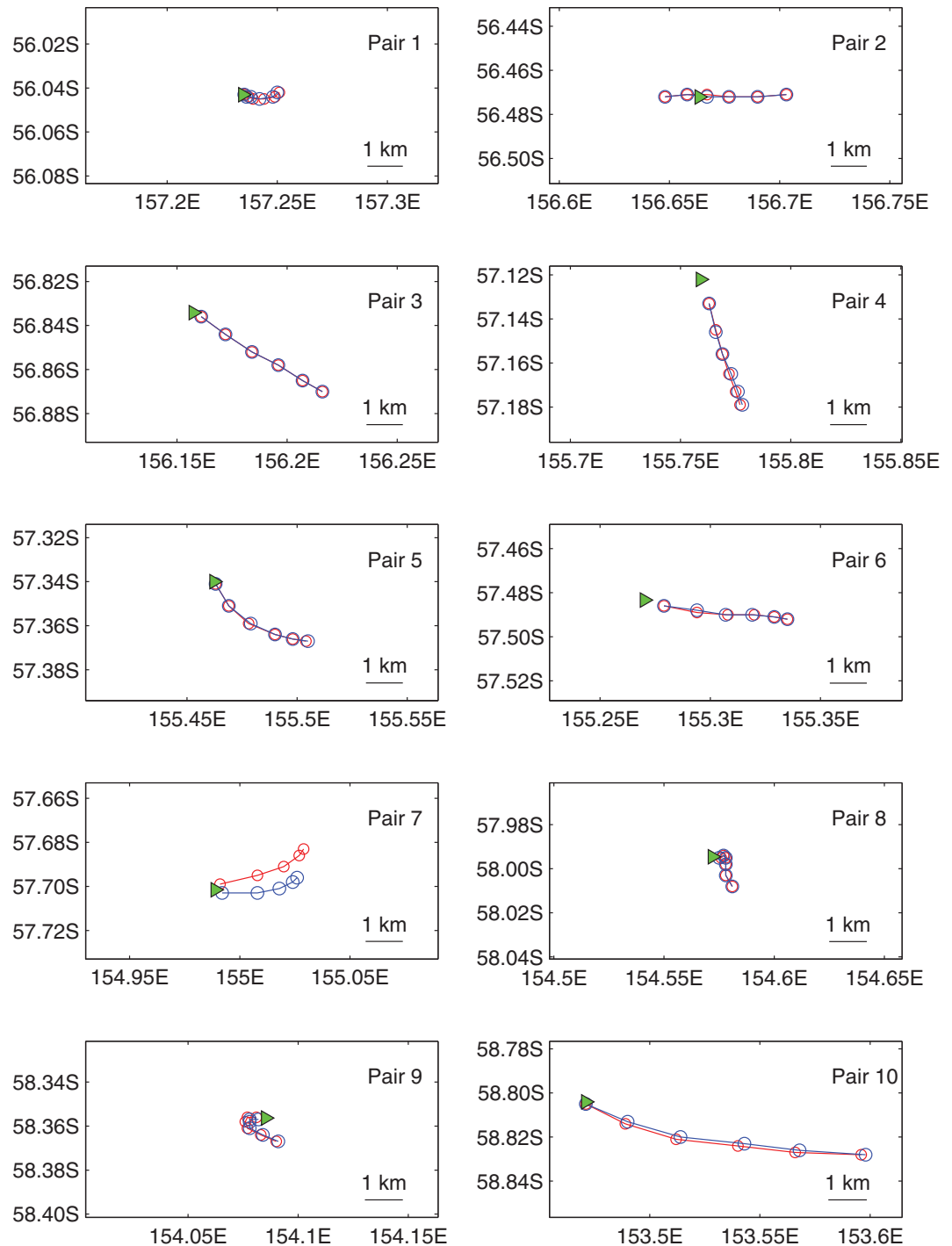


Figure 6. Drifter trajectories during the first 5 h after release for each of the 10 pairs of AAE drifters. The start locations are given by the green triangles, and the hourly positions of the drifters in the pair are given by the red and blue circles. Zonal and meridional scales are equal for each plot, and the black lines in the lower-right corner represent 1 km distance. Clearly, pair 7 stands out from the rest in that the two drifters were already separated by a few hundred meters upon the first location fix.

distance from the jet core (Figure 7a, inset). This could indicate that our sample size was not sufficiently large, that we did not sample the different parts of the front well enough, or that there is no clear cross-frontal variation in dispersion across this part of the ACC. If this latter statement is true, these results are in contrast to the varying relative cross-jet dispersion distribution reported by *Sallée et al.* [2011].

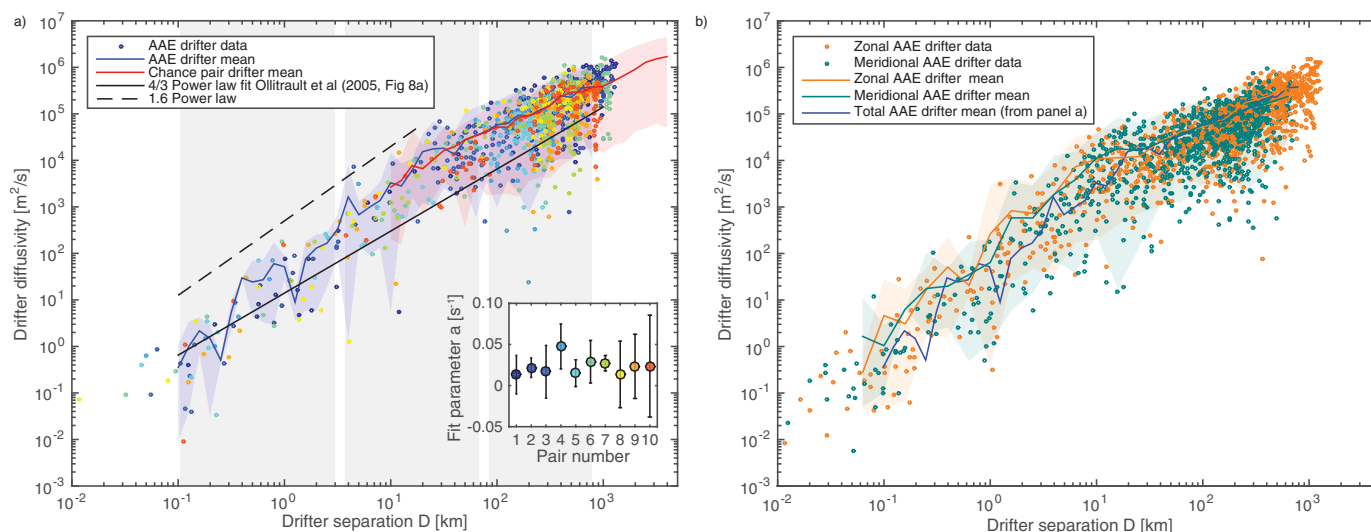


Figure 7. Diffusivity as a function of drifter separation for the 10 AAE pairs. (a) The drifters are color coded by their release latitude, see Figure 1. (b) The diffusivity is split into the zonal direction (orange) and the meridional direction (green). The mean of the AAE drifters is shown by the thick blue line, with the envelope indicating the 95% range of the data spread. The mean and 95% spread of the 12 chance pairs are shown in red, and agree very well with the data from the AAE pairs. The solid black line is the theoretical Richardson $D^{4/3}$ power law [Richardson, 1926], the dashed black line is the $D^{1.6}$ power law that better fits the observed diffusivity on small scales ($D < 20$ km). The light grey areas are the three regimes identified by the FSLE analysis. The inset shows the fit parameter a_i for a power law with exponent 1.6 for each of the individual pairs i .

4. Conclusions

Using 10 pairs of surface drifters deployed in the southwest Pacific sector of the Southern Ocean across the SACCF on the 2013/2014 Australasian Antarctic Expedition, augmented with 12 independent chance pairs from the NOAA archive, we report the first direct quantification of submesoscale and mesoscale pairwise drifter dispersion and derived diffusivity in the Southern Ocean.

Our FSLE analysis identifies two regimes in the submesoscale below approximately twice the Rossby radius of deformation, with a regime transition around the 3 km scale. For scales larger than this scale, both the FSLE and dispersion characteristics suggest a mixed QG/SQG flow. For scales smaller than 3.2 km, however, the FSLE analysis suggests Richardson's Law behavior, while the dispersion analysis suggests an exponential regime.

While many studies report a regime transition within the submesoscale, the dynamics attributed to the two regimes are often different, with studies reporting ballistic, Richardson, and exponential dispersion. Here we show that even within a single data set the interpretation of the regimes can be complicated, as the slopes of the FSLE and the dispersion versus time analysis do not always agree (Figure 3 versus Figure 5a). While the characterization of the regime behavior between 3.2 and 73 km seems robust in both analyses, the characterization of the regime for scales less than 3.2 km is very different in the FSLE analysis compared with the dispersion analysis. This discrepancy between different diagnostics is not uncommon or unexpected, and is consistent with emerging evidence that inertial oscillations can contaminate FSLE on very small scales (Beron-Vera and LaCasce, manuscript in preparation).

The analysis of diffusivity shows that in the AAE data, the diffusivity is scale-dependent down to 100 m, following a power law relationship with an exponent value between the Richardson exponent of $4/3$ and 1.6. This means that, at least in this region, tracer stirring is local rather than nonlocal; that is, stirring on small scales is controlled by small-scale eddies rather than the mesoscale flow. This has interesting implications for numerical ocean models where subgrid-scale diffusion of tracers is often implicitly assumed to be governed by a large-scale straining field, in which pair dispersion grows exponentially with time [Batchelor, 1952]. Our results suggest that a more sophisticated approach is needed to accurately model submesoscale dispersion in this region [Poje et al., 2010; Le Sommer et al., 2011].

Our analysis also finds that the diffusivity appears to be more isotropic than expected, with no significant difference between the zonal and meridional components. While, ideally, this separation should have been

done into along-stream and cross-stream diffusivity to truly test the degree of anisotropy, this is difficult with data on much smaller scales than the satellite products provide.

In general, pairwise drifter diffusivity literature is often contradictory, making intercomparisons between regions extremely difficult. Part of this disagreement may be from differences in ocean dynamics between regions or differences in sea state. In our case, the calm summer conditions might mean that mixed-layer instabilities play a relatively minor role in surface dispersion compared to say in the wintertime North Atlantic, and the presence of submesoscale motions may be relatively limited as a result. However, much of the discrepancy between studies may also be due to different deployment strategies, drifter designs, and perhaps even the low number of pairs included in the analysis, as our outlier issue clearly illustrates.

Acknowledgments

This work was supported by the Australasian Antarctic Expedition 2013–2014, the Australian Research Council (DE130101336, DE120102927, FL100100195, FT120100004, and DP130104156), and the University of New South Wales. R.L. received support from NOAA's Climate Program Office and the Atlantic Oceanographic and Meteorological Laboratory (AOML). We thank Shaun Dolk and Erik Valdez at the NOAA AOML GDP for their help with the drifters and data and members of the AAE 2013–2014 for the deployment of the drifters. The trajectories of the 2013/2014 AAE drifters are available through the NOAA GDP Drifter Data Assembly Center (<http://www.aoml.noaa.gov/phod/dac/dacdata.php>). The altimeter products were produced by Ssalto/Duacs and distributed by Aviso, with support from CNES (<http://www.aviso.oceanobs.com/duacs/>). MODIS Aqua sea-surface temperature data are distributed by NASA (<http://oceancolor.gsfc.nasa.gov>). Insightful comments by Joe LaCasce and two anonymous reviewers proved extremely valuable.

References

- Batchelor, G. K. (1952), The effect of homogeneous turbulence on material lines and surfaces, *Proc. R. Soc. London, Ser. A*, *213*, 349–366, doi:10.1098/rspa.1952.0130.
- Bennett, A. F. (1984), Relative dispersion—Local and nonlocal dynamics, *J. Atmos. Sci.*, *41*, 1881–1886.
- Berti, S., F. A. D. Santos, G. Lacorata, and A. Vulpiani (2011), Lagrangian drifter dispersion in the southwestern Atlantic Ocean, *J. Phys. Oceanogr.*, *41*(9), 1659–1672, doi:10.1175/2011JPO4541.1.
- Chelton, D. B., R. A. DeSzoeke, M. G. Schlax, K. El Naggar, and N. Siwertz (1998), Geographical variability of the first baroclinic Rossby radius of deformation, *J. Phys. Oceanogr.*, *28*(3), 433–460, doi:10.1175/1520-0485(1998)028<0433:GVOTFB>2.0.CO;2.
- Chelton, D. B., M. G. Schlax, R. M. Samelson, and R. A. de Szoeke (2007), Global observations of large oceanic eddies, *Geophys. Res. Lett.*, *34*, L15606, doi:10.1029/2007GL030812.
- Davis, R. E. (1985), Drifter observations of coastal surface currents during CODE: The statistical and dynamical views, *J. Geophys. Res.*, *90*, 4756–4772.
- Early, J. J., R. M. Samelson, and D. B. Chelton (2011), The evolution and propagation of quasigeostrophic ocean eddies, *J. Phys. Oceanogr.*, *41*, 1535–1555.
- Ferrari, R., and M. Nikurashin (2010), Suppression of eddy diffusivity across jets in the Southern Ocean, *J. Phys. Oceanogr.*, *40*(7), 1501–1519, doi:10.1175/2010JPO4278.1.
- Haza, A. C., A. C. Poje, T. M. Özgökmen, and P. J. Martin (2008), Relative dispersion from a high-resolution coastal model of the Adriatic Sea, *Ocean Modell.*, *22*, 48–65, doi:10.1016/j.ocemod.2008.01.006.
- Haza, A. C., T. M. Özgökmen, A. Griffa, A. Molcard, P.-M. Poulain, and G. Peggion (2010), Transport properties in small-scale coastal flows: Relative dispersion from VHF radar measurements in the Gulf of La Spezia, *Ocean Dyn.*, *60*(4), 861–882, doi:10.1007/s10236-010-0301-7.
- Haza, A. C., T. M. Özgökmen, A. Griffa, A. C. Poje, and M. P. Lelong (2014), How does drifter position uncertainty affect ocean dispersion estimates? *J. Atmos. Oceanic Technol.*, *31*(12), 2809–2828, doi:10.1175/JTECH-D-14-00107.1.
- Held, I. M., R. T. Pierrehumbert, S. T. Garner, and K. L. Swanson (1995), Surface quasi-geostrophic dynamics, *J. Fluid Mech.*, *282*, 1–20, doi:10.1017/S0022112095000012.
- Hellweger, F. L., E. van Sebille, and N. D. Fredrick (2014), Biogeographic patterns in ocean microbes emerge in a neutral agent-based model, *Science*, *345*, 1346–1349, doi:10.1126/science.1254421.
- Kamenkovich, I., I. I. Rypina, and P. S. Berloff (2015), Properties and origins of the anisotropic eddy-induced transport in the North Atlantic, *J. Phys. Oceanogr.*, *45*(3), 778–791, doi:10.1175/JPO-D-14-0164.1.
- Kirwan, A. D., Jr., G. J. McNally, E. Reyna, and W. J. Merrell Jr. (1978), The near-surface circulation of the eastern North Pacific, *J. Phys. Oceanogr.*, *8*(6), 937–945, doi:10.1175/1520-0485(1978)008<0937:TNSCOT>2.0.CO;2.
- Klocker, A., and R. Abernathey (2014), Global patterns of mesoscale eddy properties and diffusivities, *J. Phys. Oceanogr.*, *44*(3), 1030–1046, doi:10.1175/JPO-D-13-0159.1.
- Koszalka, I., J. H. LaCasce, and K. A. Orvik (2009), Relative dispersion in the Nordic Seas, *J. Mar. Res.*, *67*(4), 411–433.
- LaCasce, J. H. (2008), Statistics from Lagrangian observations, *Prog. Oceanogr.*, *77*(1), 1–29, doi:10.1016/j.pocan.2008.02.002.
- LaCasce, J. H., and J. C. Ohlmann (2003), Relative dispersion at the surface of the Gulf of Mexico, *J. Mar. Res.*, *61*(3), 285–312.
- Lacorata, G., E. Aurell, and A. Vulpiani (2001), Drifter dispersion in the Adriatic Sea: Lagrangian data and chaotic model, *Ann. Geophys.*, *19*(1), 121–129.
- Lapeyre, G., and P. Klein (2006), Dynamics of the upper oceanic layers in terms of surface quasigeostrophy theory, *J. Phys. Oceanogr.*, *36*, 165–176, doi:10.1175/JPO2840.1.
- Le Sommer, J., F. d'Ovidio, and G. Madec (2011), Parameterization of subgrid stirring in eddy resolving ocean models. Part 1: Theory and diagnostics, *Ocean Modell.*, *39*(1–2), 154–169, doi:10.1016/j.ocemod.2011.03.007.
- Lumpkin, R., and S. Elipot (2010), Surface drifter pair spreading in the North Atlantic, *J. Geophys. Res.*, *115*, C12017, doi:10.1029/2010JC006338.
- Lumpkin, R., and M. Pazos (2007), *Lagrangian Analysis and Prediction of Coastal and Ocean Dynamics*, edited by A. Griffa et al., Cambridge Univ. Press, Cambridge, U. K.
- Mazloff, M. R., P. Heimbach, and C. Wunsch (2010), An eddy-permitting Southern Ocean state estimate, *J. Phys. Oceanogr.*, *40*(5), 880–899, doi:10.1175/2009JPO4236.1.
- Naveira Garabato, A. C., R. Ferrari, and K. L. Polzin (2011), Eddy stirring in the Southern Ocean, *J. Geophys. Res.*, *116*, C09019, doi:10.1029/2010JC006818.
- Ohlmann, J. C., and P. P. Niiler (2001), A two-dimensional response to a tropical storm on the Gulf of Mexico shelf, *J. Mar. Syst.*, *29*(1–4), 87–99.
- Ollitrault, M., C. Gabillet, and A. C. De Verdiere (2005), Open ocean regimes of relative dispersion, *J. Fluid Mech.*, *533*, 381–407, doi:10.1017/S0022112005004556.
- Pedlosky, J. (1987), *Geophysical Fluid Dynamics*, Springer, Springer-Verlag, N. Y.
- Poje, A. C., A. C. Haza, T. M. Özgökmen, M. G. Magaldi, and Z. D. Garraffo (2010), Resolution dependent relative dispersion statistics in a hierarchy of ocean models, *Ocean Modell.*, *31*(1–2), 36–50, doi:10.1016/j.ocemod.2009.09.002.
- Poje, A. C., et al. (2014), Submesoscale dispersion in the vicinity of the Deepwater Horizon spill, *Proc. Natl. Acad. Sci. U. S. A.*, *111*(35), 12,693–12,698, doi:10.1073/pnas.1402452111.

- Richardson, L. F. (1926), Atmospheric diffusion shown on a distance-neighbour graph, *Proc. R. Soc. London, Ser. A*, 110(756), 709–737.
- Rintoul, S. R., and A. C. Naveira Garabato (2013), Dynamics of the Southern Ocean circulation, in *Ocean Circulation and Climate—A 21st Century Perspective*, edited by G. Siedler et al., pp. 471–492, Elsevier, Oxford, U. K.
- Sallée, J.-B., K. Speer, R. Morrow, and R. Lumpkin (2008), An estimate of Lagrangian eddy statistics and diffusion in the mixed layer of the Southern Ocean, *J. Mar. Res.*, 66(4), 441–463.
- Sallée, J.-B., K. Speer, and S. R. Rintoul (2011), Mean-flow and topographic control on surface eddy-mixing in the Southern Ocean, *J. Mar. Res.*, 69(4-6), 4–6.
- Salmon, R. (1998), *Lectures on Geophysical Fluid Dynamics*, Oxford Univ. Press, Oxford, U. K.
- Schroeder, K., A. C. Haza, A. Griffa, T. M. Ozgokmen, P. M. Poulain, R. Gerin, G. Peggion, and M. Rixen (2011), Relative dispersion in the Liguro-Provençal basin from sub-mesoscale to mesoscale, *Deep Sea Res., Part I*, 58(3), 209–228, doi:10.1016/j.dsr.2010.11.004.
- Schroeder, K., et al. (2012), Targeted Lagrangian sampling of submesoscale dispersion at a coastal frontal zone, *Geophys. Res. Lett.*, 39, L11608, doi:10.1029/2012GL051879.
- Stammer, D. (1998), On eddy characteristics, eddy transports, and mean flow properties, *J. Phys. Oceanogr.*, 28(4), 727–739.
- Taylor, G. I. (1921), Diffusion by continuous movements, *Proceedings of the London Mathematical Society*, 20, 196–211, doi:10.1234/12345678.
- Trani, M., P. Falco, E. Zambianchi, and J.-B. Sallée (2014), Aspects of the Antarctic Circumpolar Current dynamics investigated with drifter data, *Prog. Oceanogr.*, 125, 1–15, doi:10.1016/j.pocean.2014.05.001.
- Tulloch, R., and K. S. Smith (2009), Quasigeostrophic turbulence with explicit surface dynamics: Application to the atmospheric energy spectrum, *J. Atmos. Sci.*, 66, 450–467, doi:10.1175/2008JAS2653.1.
- Vallis, G. K. (2006), *Atmospheric and Oceanic Fluid Dynamics*, Cambridge Univ. Press, Cambridge, U. K.
- van Sebille, E., M. H. England, and G. Froyland (2012), Origin, dynamics and evolution of ocean garbage patches from observed surface drifters, *Environ. Res. Lett.*, 7(4), 044040, doi:10.1088/1748-9326/7/4/044040.
- Zhurbas, V. (2004), Drifter-derived maps of lateral diffusivity in the Pacific and Atlantic Oceans in relation to surface circulation patterns, *J. Geophys. Res.*, 109, C05015, doi:10.1029/2003JC002241.